Direct Thrust and Velocity Measurement for a Micro UAV Rotor

Edwin Davis, Paul EI Pounds*
University of Queensland, Australia
{firstname.lastname}@uq.edu.au

Abstract

Thrust and velocity sensing is very important for the control of micro UAVs. Contemporary high-performance quadrotor motion control relies on accurate high-speed trajectory sensing. However, position and velocity sensing is challenging outside of an indoor Vicon arena: GPS is slow and noisy, optical flow sensors do not work far from ground, and pitot tubes perform poorly at low speeds.

Our approach is to use a compact force-torque sensor to directly measure rotor forces and pitch-roll torques. The sensor is constructed from MEMS barometers encapsulated in an elastic compound, attached to a load plate. The sensor can provide sub-mN thrust force sensing at 1 kHz, with torque sensitivity better than 0.1 mN·m. Using a lumped parameter model of rotor induced drag and flapping torque-velocity coupling, we can accurately estimate translational velocity of a rotor. The velocity output is linear for translational velocities from below 0.25 to over 0.8 ms^{-1}.

1 Introduction

Precision flight control of miniature robot aircraft requires an accurate model of vehicle dynamics and the forces acting upon it [Mellinger *et al*, 2012]. However, the principle source of force applied to a multirotor aircraft — its rotor — provides a variable amount of force depending upon the local aerodynamic conditions, proximity of objects and the manoeuvres of the aircraft [Davis *et al*, 2015]. As a consequence, typical control approaches rely on very accurate and high-speed sensing of trajectory, using onboard MEMS intertial measurement units (IMUs) and systems such as Vicon, to detect and correct for deviation induced by disturbances or by errors in the rotor actuation model. Unfortunately, low-cost accelerometers are not accurate enough for precision dead-reckoning and precision IR tracking tools are not effective outdoors due to insolation.

Figure 1: Force sensor mounted under motor.

Other sensors are not able to fill the gap: GPS is slow and noisy, optical flow sensors do not function far from ground, and pitot tubes do not function well at low speeds. While barometers are generally effective for altitude measurement within ±100 mm, there is currently no effective lateral velocity sensor.

An alternative approach is to focus on improving the dynamic model of the aircraft and estimate the internal states of the rotor, so as to improve trajectory tracking in the framework of less capable sensors. Bangura and Mahony use a sophisticated rotor model, combined with a motor power sensor and estimator to estimate the rotor force and lateral velocity [Bangura and Mahony, 2012] [Bangura and Mahony, 2014] [Bangura *et al*, 2015]. However, this requires access to the electronic speed controller internals, and high-speed processing.

*Corresponding author. This work is supported by Australian Research Council grant DE130100885.

Our approach is to instead directly sense the force and transverse torques generated at the rotor, to feed into the dynamic model of the aircraft. In this way, irrespective of the local aerodynamic conditions of the rotor, the correct desired thrust may always be applied through a tight feedback control loop. Furthermore, by exploiting the known coupled mechanics between rotorcraft translation and pitch velocity through induced drag and flapping, we can construct a direct measurement of the speed of the aircraft.

In this paper we present a novel rotor thrust and transverse torque sensor that can measure the axial and off-axis thrust of the rotor. In Section 2 we describe the construction and function of the sensor. In Section 3 we derive a simple lumped parameter model for translating transverse thrust components into an estimate of translational velocity. In Section 4 we present experiments verifying the sensitivity and linearity of the sensor when mounted on a rotating velocity test-rig. In Section 5 we discuss the features, performance and applications of the sensor, based on the measured results, and a brief conclusion completes the paper.

2 Force Sensor

We developed a lightweight and low cost motor force sensor capable of measuring one lift force and two transverse rotor torques of a small BLDC (Brushless DC) rotor system. The design leverages the technique developed at Harvard for using low-cost MEMS barometers as tactile force sensors by encasing them in polyurethane rubber [Tenzer *et al*, 2014]. The Harvard, and later Right Hand Robotics "Takktile", sensors use Freescale MPL115A2 MEMS barometers which feature a large opening in the case directly above the silicon sensing element. These sensor arrays can measure tactile contact forces with a sensitivity of 1 g. We build upon this technique by using a small array of potted sensors as the elements of a miniature load cell.

2.1 Construction

The force sensor is comprised of four sensors, a microcontroller and USB connection mounted to a PCB (Printed Circuit Board). Four threaded stand-offs are soldered to the PCB for securing the sensor the the quadrotor. An acrylic load plate is glued to the top of the polyurethane encased pressure sensors and retains four captive screws for attaching the motor. The complete sensor is shown in Figures 2 and 3. The completed sensor mass is 3 g.

It was found that the MPL115A2 sensors sensors did not offer sufficient resolution for accurately measuring small motor forces. Instead we use the Measurement Specialties MS5611, which offers two orders of magnitude improvement in resolution and nearly triple the maximum sampling frequency at up to 1.8 kHz.

During operation the sensors heat up, causing the rubber to expand against the sensing element and rapidly saturate device. This was due to the incompressible nature of the polyurethane rubber and the lack of a large opening in the stainless steel cap above the sensor for the rubber to expand out of. To improve sensitivity we de-capped the MS5611 sensor by forcibly removing the stainless steel case to directly expose the MEMS sensor die. It was found that the rotor pulling on the rubber sensor mounts gave better reading than compressing them.

An effective method for moulding the Smooth-on Vytaflex 20 polyurethane over the sensors is to use a mould that was laser cut out of acrylic and screwed to PCB through the threaded stand-offs. A second piece of acrylic was used as a lid to cover the top of the sensor moulds and pressed down to displace the excess polyurethane and produce moulded parts of uniform thickness with a smooth glass like top surface. A thin smear of petroleum jelly was applied to the acrylic mould parts to act as a release agent.

The total bill of materials cost per sensor is approximately $50 in quantities of 10.

2.2 Force Model

An arrangement of four pressure sensors in a square allows for independent measurement of the torques along each diagonal by taking the difference of two opposite sensor readings. The thrust produced by the motor can be computed by taking the sum of all four scaled sensor readings.

The force F_n on each sensor element approximated as a simple spring is given by:

$$F_n = k\bar{p}_n \tag{1}$$

where k is the sensor coefficient and $\bar{p}_n$ is the tared sensor reading under gauge load given by $\bar{p}_n = p_n - p_{n0}$.

The total vertical force F_z measured by the die sensor array is given by:

$$F_z = \sum F_n \tag{2}$$

$$F_z = k(\bar{p}_1 + \bar{p}_2 + \bar{p}_3 + \bar{p}_4) \tag{3}$$

The torques τ_x and τ_y measured by the motor force sensor are given by:

$$\tau_x = kd(\bar{p}_1 - \bar{p}_3) \tag{4}$$

$$\tau_y = kd(\bar{p}_2 - \bar{p}_4) \tag{5}$$

where d is the horizontal distance of the sensing elements from the central of the motor force sensor.

The sensor coefficient was determined by loading the sensor with a series of known masses and found to be $k = 3058$ units/N.

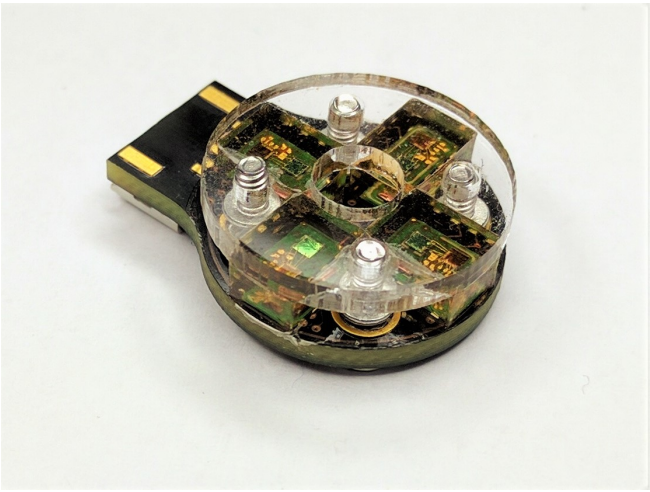

Figure 2: Assembled force sensor front.

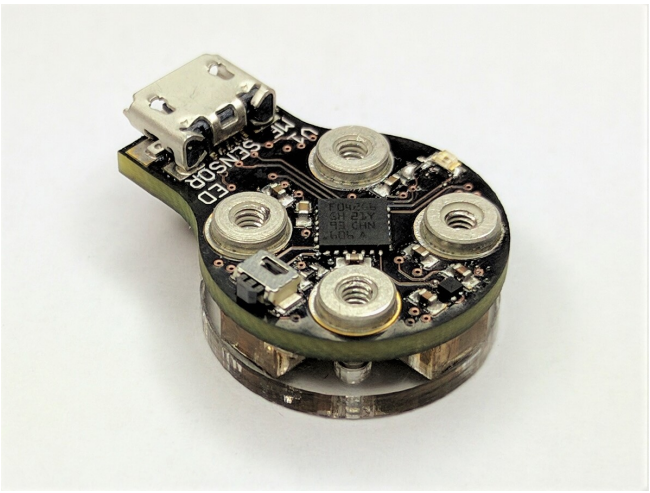

Figure 3: Assembled force sensor back.

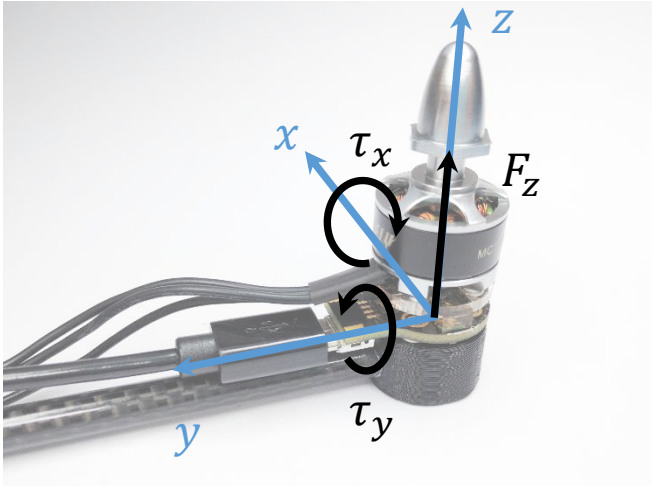

Figure 4: Mounted sensor with reference frame and vectors.

2.3 Sensor Comparison

To test the performance of the motor force sensor it was attached to a test rig as shown in Figure 5 along with a $5000 JR3 force torque sensor for comparison. The JR3 6-DOF force torque sensor is attached the the bench. Because the JR3 sensor is designed to measure much larger forces and has a lower resolution a force multiplying arm was used to improve sensitivity. The motor and sensor were attached to the end of this arm. In place of a rotor a pulley and suspended cup were attached to the motor shaft. A single point calibration of both the JR3 and motor force sensor were performed using a known mass and measuring the offsets from sensor centres. After taring the sensor readings a water bottle was used to gradually fill the cup while time stamped sensor measurements were recorded at 190 Hz for the JR3 and 1000 Hz for the force sensor. For comparison purposes the JR3 readings were scaled by the ratio of the lever arms, 1.01 $m/0.022$ $m = 49.5$. The JR3 force torque sensor was filtered using a built in 125 Hz low-pass filter. No filtering was applied to the motor force sensor. The comparison results are shown in Figure 6.

The result show that the motor force sensor accurately tracks the torque as measured by the substantially more expensive JR3. There are some oscillations in the JR3 readings which are likely due to the experimental setup. As the cup is filled it begins to bounce around on the end of the lever arm which bends and transmits the motion into the JR3 sensor at the base, the motor force sensor moves with the cup.

3 Velocity Torque Model

When a horizontal rotor is translating sideways with some velocity, induced drag and blade flapping cause the rotor to apply a component of force against the direction of travel [Martin and Salaün, 2010] [Pounds *et al*, 2010]. The horizontal force subtends a torque about the vertical offset between the rotor plane and load plate which can be measured by the load cell.

The free body diagram of a simplified planar model comprised of two sensing elements is considered as shown in Figure 7. The force sensors are compressible and allow small deflections under load.

We treat the action of blade flapping and induced drag as an effective force vector deflection given by:

$$T_x = T(q_1\dot{x} - q_2\dot{\theta}) \tag{6}$$

where q_1 and q_2 are the lumped translational and pitch velocity coefficients, $\dot{x}$ is the longitudinal velocity of the rotor and $\dot{\theta}$ is the pitch velocity.

In dynamic maneuvers, this value may be measured by a precision gyro and cancelled; in quasi static hovering flight, $\dot{\theta} \approx 0$. The component of thrust directed

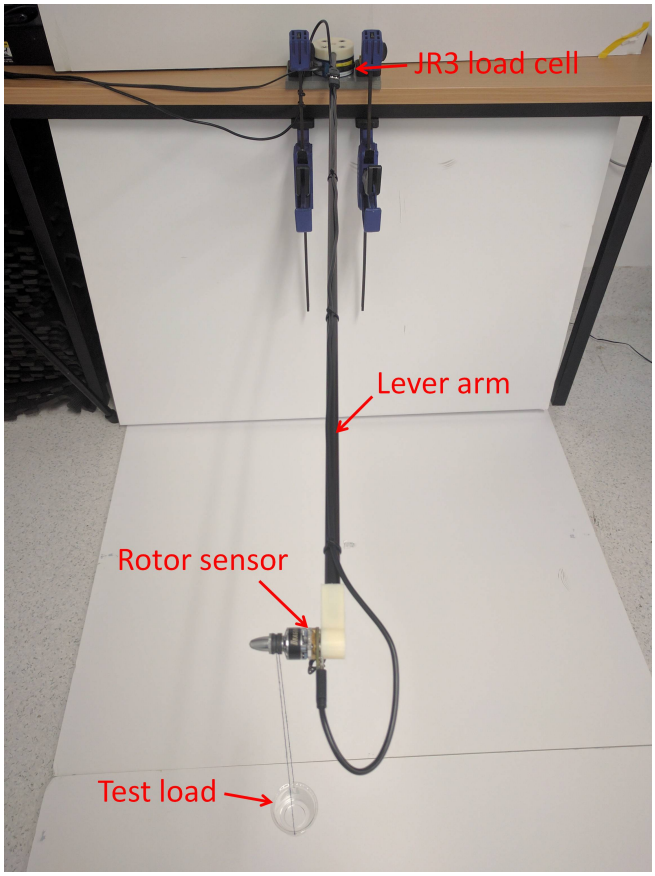

Figure 5: Static force sensor and JR3 load cell apparatus for torque comparison test.

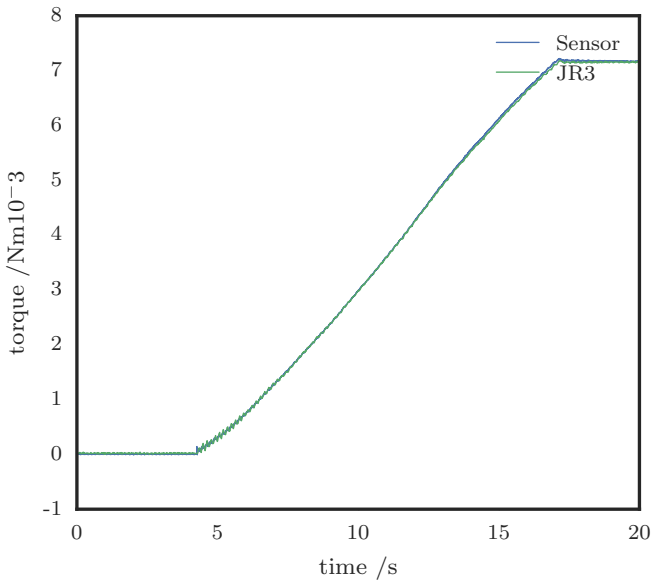

Figure 6: Force sensor comparison with JR3 load cell.

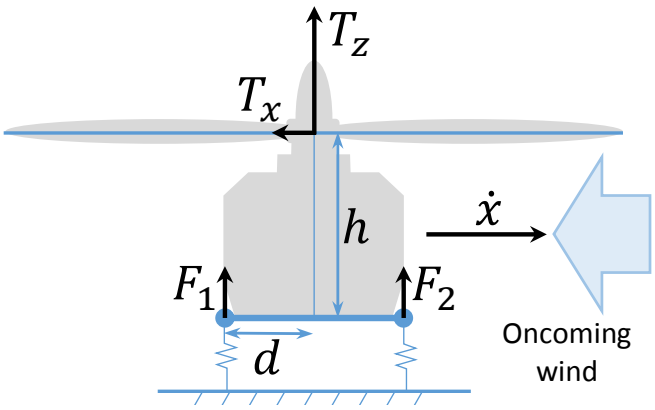

Figure 7: System free body diagram.

into the horizontal by induced drag and blade flapping is therefore given by:

$$T_x = (F_1 + F_2) q_1 \dot{x} \tag{7}$$

Under load the motor rotor system will tilt to some static equilibrium in which the torques around the centre of rotation will be equal:

$$T q_1 \dot{x} h = d \Delta F \tag{8}$$

$$\dot{x} = \frac{d}{q_1 h} \frac{\Delta F}{T} \tag{9}$$

$$\dot{x} = \frac{d}{q_1 h} \frac{F_1 - F_2}{F_1 + F_2} \tag{10}$$

where h is the height of the rotor aerodynamic centre above the centre of rotation, d is the horizontal distance of the sensor element from the centre of rotation, ΔF is the difference between the sensor element forces, F_1 and F_2 are the individual sensor element forces.

Using this relation, the sensor measurements may be used to compute an estimate of $\dot{x}$. Parameters for the motor, rotor and prototype sensor are given in Table 1.

4 Lateral Velocity Experiments

A series of experiments were carried out to characterise the rotor-motor-sensor system and determine the effectiveness of the force sensor in measuring the lateral velocity of a rotor. Basic testing to demonstrate the function of the force measurement elements was trivial, and is not included here.

The validation of the lateral sensing function required accurate replication of steady, constant-velocity motion.

Table 1: Sensor, Motor and Rotor Parameters.

d	sensor offset	0.0045	m
h	rotor height offset	0.02	m
k	sensor coefficient	3058	units/N
q_1	rotor coefficient	0.138	s/m

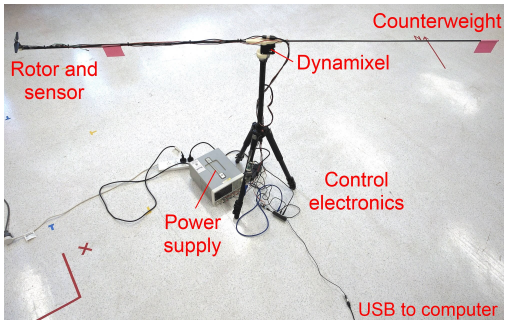

Figure 8: Swing-arm apparatus.

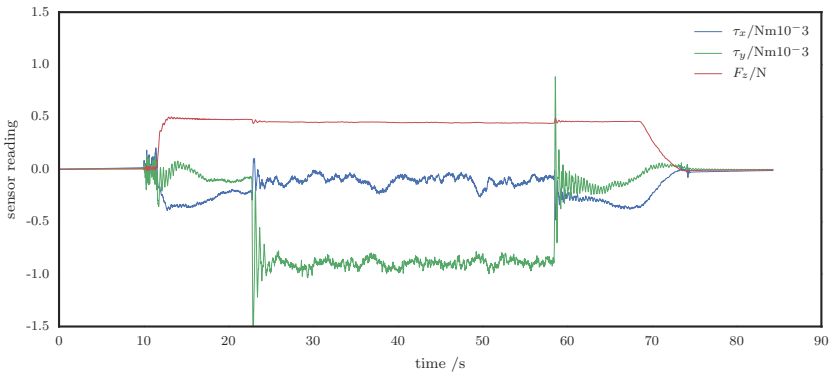

Figure 9: Exemplar sensor measurement, $\dot{x} = -0.53$ ms^{-1}.

We constructed a long swing-arm mechanism to move a rotor through a circular arc, approximating linear motion. The arm is a 1 m long, 6 mm diameter woven carbon fibre tube, attached to a Dynamixel MX64 motor mounted to a tripod. The motor is a Dragonfly MC1306 3100 KV motor, with a T-Motor 6.5x3.5" rotor, driven by a Dys XM10A ESC powered by a 8.4 V bench supply. The motor is secured to the tube with a 3D printed mount.

The force sensor, ESC and Dynamixel were connected to a computer via USB for control and data capture. The complete experimental apparatus is shown in figure 8.

During each experiment, the sensor force and torque data was recorded at 1000 Hz starting with 10 s when the rotor and platform were stationary. The applied motor voltage was then gradually increased to 30 per cent, approximately hover thrust for a 200 g quadrotor. After 10 s of settling time, the platform started to rotate at the specified rate until it completed three revolutions, whereupon it halted. A further 10 s of data was captured with the platform stationary and the rotor still spinning before the rotor was brought to a stop. A final 10 s of sensor data was recorded before the experiment was concluded.

An exemplar test of the sensor moving with a tangential velocity of -0.53 ms^{-1} is shown in figure 9.

Four translation sensing experiments were undertaken: a control test with the rotor stationary, rotation of the swing-arm clockwise and counter-clockwise, operation of the sensor with and without air conditioning active, and a set of tests to establish the linearity of the sensor.

4.1 Sensing with Clockwise and Counter-Clockwise Arm Rotation

To determine the effect of platform rotation direction on the sensor measurements, two tests were conducted with the swing-arm rotating first counter-clockwise and then clockwise — see figures 10a and 10b. When rotating counter-clockwise, the torque τ_y was positive; when rotating clockwise at the same speed it was of similar magnitude and negative, as expected. The tangential velocity of the rotor during each test was -0.66 ms^{-1} and 0.66 ms^{-1} for counter-clockwise and clockwise swings, respectively.

Contrary to expectations, F_z was observed to increase slightly during counter-clockwise swing-arm rotation, but decrease in clockwise rotation — a total change of less than 5 per cent. A 10 Hz filter was applied to the sensor data to make this offset more apparent. It is not clear if this effect reflects an actual change in the measured thrust value, or an artifact of the sensor or testing apparatus. A mutual increase could be explained by translational lift of the rotor, but a change in opposing direction must have a different explanation.

The source of this difference could be narrowed down by conducting additional experiments with the rotor spinning in the opposite direction and again observing the thrust change for clockwise and counter-clockwise swing-arm rotation.

4.2 Sensor with Rotor Stationary

To determine the influence of the platform motion on the force sensor readings, an experiment was conducted without the rotor spinning. This removes the influence of aerodynamic effects, leaving only forces induced by the apparatus, as shown in Figure 11. The tangential velocity of the rotor was -0.66 ms^{-1}.

This shows the coupling of the platform arm movement into the sensor readings — in particular the high-frequency transients at the beginning and end of motion. This is believed to be due to torsional oscillation of the high-mounted motor weight about the axis of the tube, excited by the step change in Dynamixel velocity.

4.3 Effect of Air Conditioning on Sensor

During initial function testing of the sensor, it was noticed that the measured rotor forces were substantially more variable and noisy than expected. We realised that the sensor is sufficiently sensitive to detect the transient aerodynamic disturbance patterns in the room induced by the laboratory air conditioning.

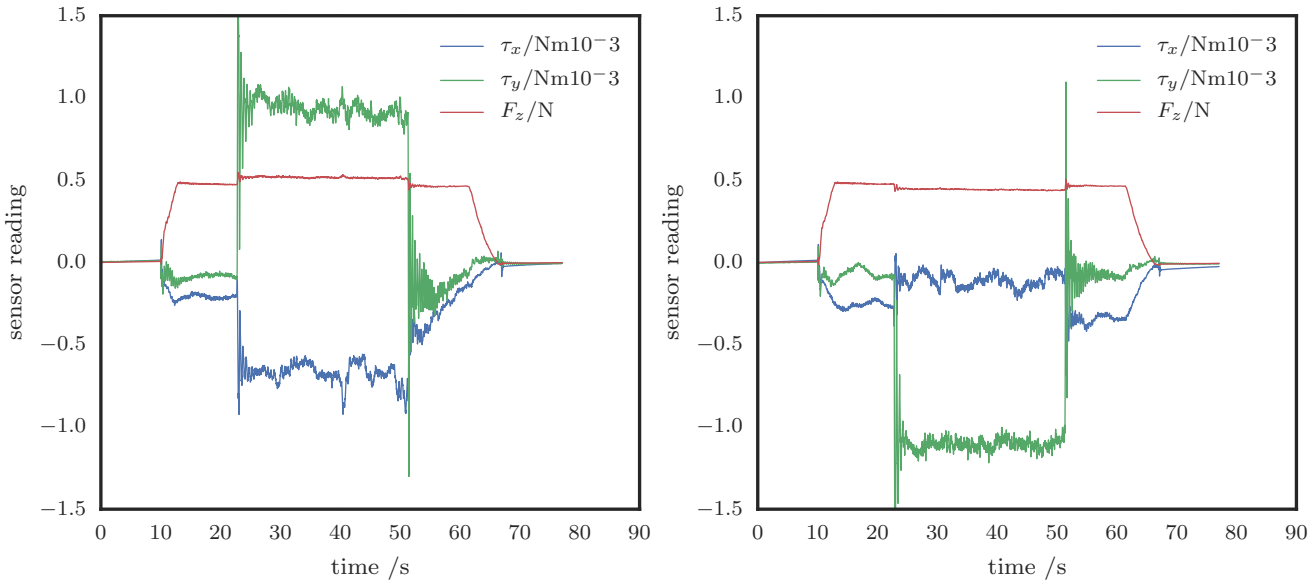

(a) CCW rotation of the platform

(b) CW rotation of the platform

Figure 10: Thrust and moment forces for motion in both directions, $\dot{x} = \pm 0.66$ ms^{-1} with a 10 Hz low pass filter applied.

Experiments were conducted with and without air conditioning on (see Fig. 12). The tangential velocity of the rotor during each arm swing was -0.53 ms^{-1}. It was found that air conditioning increased the cyclic measurement deviation in tests by a factor of ∼5 — the three oscillations in the torque measurements roughly correspond to the three revolutions of the swing-arm, and indicate that the observed variation is linked to a global ambient flow field.

To reduce the effect of these disturbances during characterisation experiments, the air conditioning was turned off for all other tests.

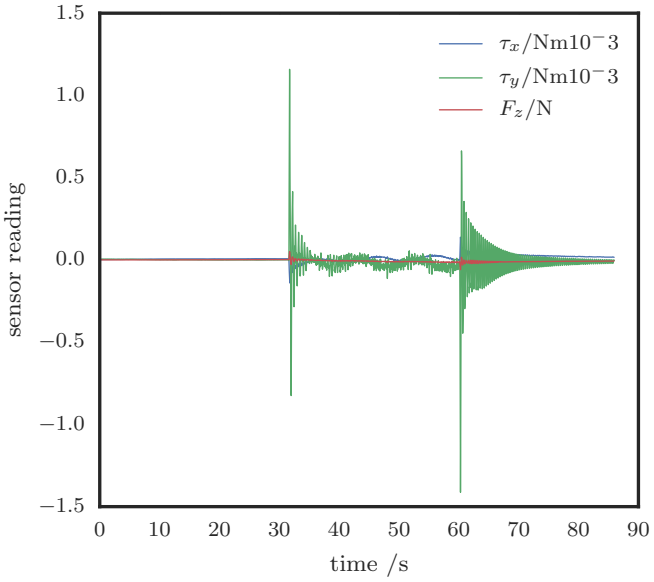

Figure 11: Sensor measurements during an experiment without the rotor spinning, $\dot{x} = -0.66$ ms^{-1}.

4.4 Velocity Sensor Linearity

To determine the linearity of the sensor for velocity estimation, an array of trials were conducted with the swing-arm set with incrementally increasing speed. This was achieved by varying the Dynamixel "moving speed" parameter from 20 to 60 units in increments of 5 units. The rotor was spinning at a constant speed near hover thrust for a 200 g micro quadrotor, providing 50 g of force. The torque measured around the radius of the platform arm, τ_y, was averaged during the middle revolution of platform and plotted against the tangential velocity of the platform in Figure 13. The plot shows a strong linear trend for the range of velocities tested (R = 0.995), and demonstrates the effectiveness of the force sensor in measuring the lateral velocity of a rotor.

5 Discussion

The sensor performed well during testing, demonstrating sufficient sensitivity to capture unintended phenomena, such as the swing-arm resonance and ambient AC flow fields. Compensating for these effects will form some of the future work of the project.

The mechanical coupling of the motor and flexible swing-arm tubes is not expected to pose a problem for applications on a micro UAV. The arms of a typical quadrotor are substantially shorter and stiffer than the shaft used. Furthermore, these types of coupled motions, and those due to pitch and roll motions in particular, can be compensated for when the sensor is combined with angular velocity measurements from the IMU.

Low speed measurements have not yet been captured for the sensor, due to the limitations of the testing ap-

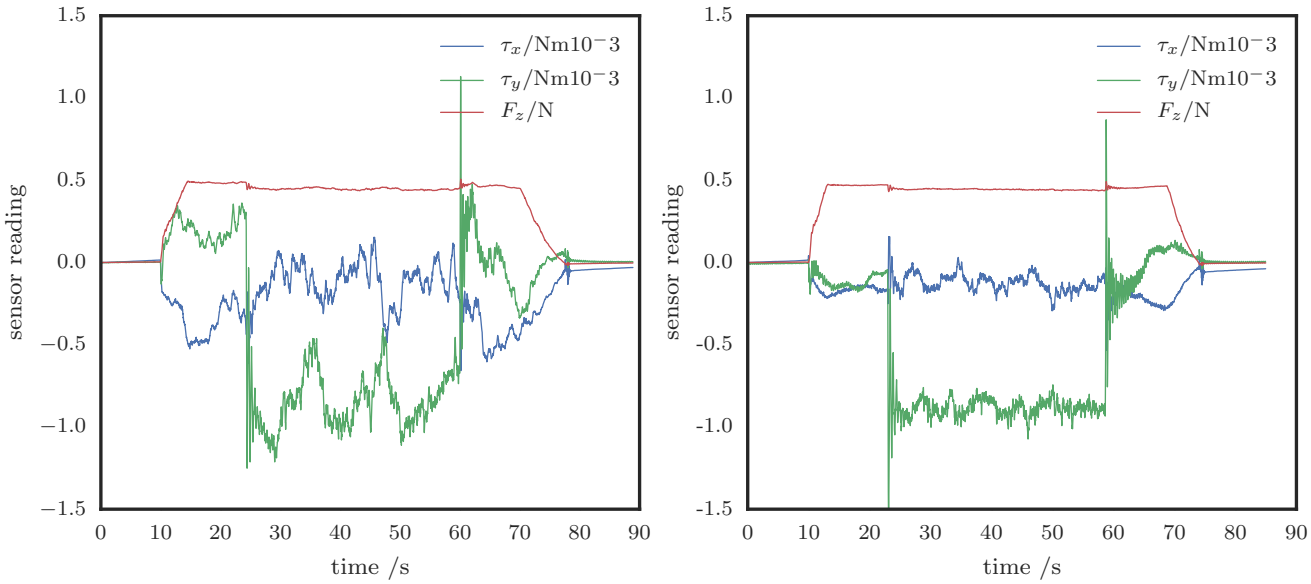

Figure 12: Thrust and moment forces with (a) and without (b) the AC turned on, both with $\dot{x} = -0.53$ ms^{-1}.

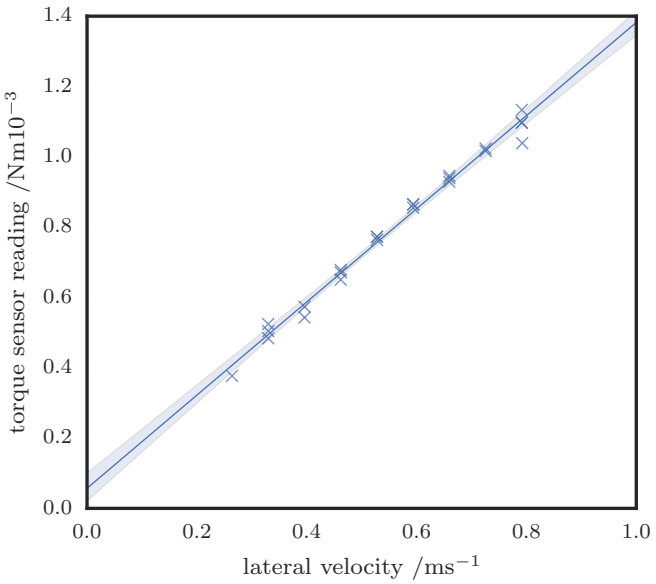

Figure 13: Torque sensor reading for varying lateral velocity of the rotor.

paratus. The current apparatus is insufficient for testing at lower velocities as the Dynamixel would oscillate instead of maintaining a constant rotation speed. A modified experimental apparatus will be developed to allow for measuring sensor performance at slower speeds.

However, it is observed that the projected intercept of the graph is not precisely zero. This is thought to be due to small offsets in the torque values that arise once the rotor is spinning. This is likely due to the sensor construction and slight rotor-sensor axial misalignment. A second calibration phase with a spinning rotor should be able to compensate for this.

The results of this paper only begin to touch the surface of the potential utility of the motor force sensors. In particular, the sensors have obvious uses for dynamic feedback control for precision manoeuvering of micro quadrotors, thrust control in ground effect and rejecting transient winds, and sensing of obstacles through their disturbance to the rotor wake field. In the near future work we will characterise the motor force sensors at lower speeds and attach them to a micro quadrotor to implement closed loop velocity control on the quadrotor using the sensors for feedback.

6 Conclusions and Future Work

We have developed a light weight motor force sensor capable of measuring thrust and lateral torques for use on a micro quadrotor UAV. Using the cross-coupling between transverse rotor torque, we were able to derive a linear mapping between sensor moment and velocity. Experimental results demonstrated that the sensor can measure the torque due to lateral velocity of a spinning

rotor producing a constant thrust of $\sim$50 g, at speeds between 0.25 and 0.8 ms^{-1}, and can measure rotor thrusts in excess of 100 g. This system has very strong promise for application in the precision dynamic control of micro UAVs.

References

[Bangura and Mahony, 2012] M. Bangura and R. Mahony. Nonlinear dynamic modeling for high performance control of a quadrotor. In *Australasian Conference on Robotics and Automation*, 2012.

[Bangura and Mahony, 2014] Moses Bangura and Robert Mahony. Real-time model predictive control for quadrotors. *IFAC Proceedings Volumes*, 2014. 19th {IFAC} World Congress.

[Bangura *et al*, 2015] M. Bangura, F. Kuipers, G. Allibert, and R. Mahony. Non-linear velocity aided attitude estimation and velocity control for quadrotors. In *Australasian Conference on Robotics and Automation*, 2015.

[Davis *et al*, 2015] E. Davis, J. Spollard, and P. Pounds. Passive height stability and trajectory repeatability of a quadrotor maneuvering in ground effect with regulated voltage bus. In *Australasian Conference on Robotics and Automation*, 2015.

[Martin and Salaün, 2010] P. Martin and E. Salaün. The true role of accelerometer feedback in quadrotor control. In *Robotics and Automation, 2010 IEEE International Conference on*, 2010.

[Mellinger *et al*, 2012] D. Mellinger, N. Michael, and V. Kumar. Trajectory generation and control for precise aggressive maneuvers with quadrotors. *The International Journal of Robotics Research*, 2012.

[Pounds *et al*, 2010] P. Pounds, R. Mahony, and P. Corke. Modelling and control of a large quadrotor robot. *Control Engineering Practice*, 2010.

[Tenzer *et al*, 2014] Y. Tenzer, L. P. Jentoft, and R. D. Howe. The feel of mems barometers: Inexpensive and easily customized tactile array sensors. *IEEE Robotics Automation Magazine*, 2014.